

Article

Electrochemical Detection of Sulfite by Electroreduction Using a Carbon Paste Electrode Binder with N-octylpyridinium Hexafluorophosphate Ionic Liquid

Maicol Bustos Villalobos¹, José Ibarra², Leyla Gidi³, Valentina Cavieres², María Jesús Aguirre^{4,5} , Galo Ramírez^{2,5,*}  and Roxana Arce^{1,5,*}

¹ Departamento de Ciencias Químicas, Facultad de Ciencias Exactas, Universidad Andrés Bello, Av. República 275, Santiago 8370146, Chile

² Departamento de Química Inorgánica, Facultad de Química y de Farmacia, Pontificia Universidad Católica de Chile, Av. Vicuña Mackenna 4860, Santiago 7820436, Chile

³ Laboratory of Materials Science, Instituto de Química de Recursos Naturales, Universidad de Talca, Talca 3460000, Chile

⁴ Departamento de Química de Los Materiales, Facultad de Química y Biología, Universidad de Santiago de Chile, USACH, Av. L.B. O'Higgins 3363, Santiago 9170022, Chile

⁵ Millenium Institute on Green Ammonia as Energy Vector (MIGA), Av. Vicuña Mackenna 4860, Macul, Santiago 7820436, Chile

* Correspondence: gramirezj@uc.cl (G.R.); roxana.arce@unab.cl (R.A.)

Abstract: Sulfite is a widely used additive in food and beverages, and its maximum content is limited by food regulations. For this reason, determining the sulfite concentration using fast, low-cost techniques is a current challenge. This work describes the behavior of a sensor based on an electrode formed by carbon nanotubes and an ionic liquid as binder, which by electrochemical reduction, allows detecting sulfite with a detection limit of $1.6 \pm 0.05 \text{ mmol L}^{-1}$ and presents adequate sensitivity. The advantage of detecting sulfite by reduction and not by oxidation is that the presence of antioxidants such as ascorbic acid does not affect the measurement. The electrode shown here is low-cost and easy to manufacture, robust, and stable.

Keywords: sulfite reduction; carbon paste electrode; ionic liquids (IL); multi-walled carbon nanotube (MWCNT)



Citation: Villalobos, M.B.; Ibarra, J.; Gidi, L.; Cavieres, V.; Aguirre, M.J.; Ramírez, G.; Arce, R. Electrochemical Detection of Sulfite by Electroreduction Using a Carbon Paste Electrode Binder with N-octylpyridinium Hexafluorophosphate Ionic Liquid. *Catalysts* **2022**, *12*, 1675. <https://doi.org/10.3390/catal12121675>

Academic Editor: Barbara Mecheri

Received: 15 November 2022

Accepted: 16 December 2022

Published: 19 December 2022

Publisher's Note: MDPI stays neutral with regard to jurisdictional claims in published maps and institutional affiliations.



Copyright: © 2022 by the authors. Licensee MDPI, Basel, Switzerland. This article is an open access article distributed under the terms and conditions of the Creative Commons Attribution (CC BY) license (<https://creativecommons.org/licenses/by/4.0/>).

1. Introduction

Preservatives and food additives are substances that are added to some foods in small amounts with the aim of storing them for a long period of time. The use of additives and preservatives is essential to maintain its quality, healthiness, taste, appearance, and flavor for a given period [1]. Sulfite is widely used as a preservative in foods and beverages during their preparation, storage, and distribution processes [2]. The preservative power of sulfite is mainly due to its reducing capacity. This makes it an effective antioxidant that also has the ability to inhibit bacterial growth [2,3].

In some cases, the presence of sulfite in food and beverages has been associated with asthma and allergic symptoms [4–6]. Therefore, regulatory agencies set maximum allowable limits [2].

There are some available methods for detecting SO_2 and its derivatives, such as titrimetric analysis, Aspiration and Ripper reference methods and the Monier–Williams (MW) method [7–10], chemiluminescence [11], physical and chemical adsorption [12,13], spectrophotometry [14,15], ion chromatography [16,17], fluorescence [18,19], biosensors [20,21], etc. Although these methods possess highly efficient detection capabilities, their intrinsic difficulties (e.g., complex operation, high equipment costs, long response times, etc.) often limit their practical applications.

Electroanalytical techniques for the determination of sulfites arise as a simpler and more attractive alternative. The main benefits of these techniques include simplicity, lower cost instrumentation, high sensitivity, and the possibility of working with colored samples, without pretreatment of the samples [22]. In addition, compared to the traditional volumetric method (MW), electroanalytical techniques allow the number of reagents to be reduced, being more respectful with the environment.

For the most part, electroanalytical methods to determine sulfite use its oxidation as an analytical signal. Using oxidation, the sulfite concentration has been determined with a nanogold electrode on gallium-doped zinc oxide [23]. Similarly, a carbon paste electrode modified with carbon nanotubes and benzoylferrocene (BF) [24] has been used. In both cases an electrocatalytic effect was found in the oxidation of sulfite. In addition, the electro-determination of sulfite has been carried out using a carbon composite electrode modified by submicron gold particles, finding good sensitivity and precision [25]. The disadvantage of determining sulfite by oxidation is that many antioxidants, usually present in foods and beverages, can act as interferences in the measurement [3]. In this sense, the platinum electrode modified with nanostructured films of Salen-copper polymer (salicylideneimine) that electrocatalyzes sulfite oxidation can be highlighted, as a notorious decrease in potential, which allows the analysis to be determined in the presence of some interfering antioxidants [26].

An attractive way to avoid the interference of common antioxidants in foods and beverages is the selective determination of sulfite through its electrochemical reduction. The reduction of sulfite in an acid medium has been studied using glassy carbon electrodes [27]. Copper-clad gold microelectrodes [28] and glassy carbon electrodes modified with ruthenium oxide and hexacyanoferrate [29] have also been used for its reduction. In all these studies, sulfite could be determined with good selectivity and sensitivity.

Based on the above information, it is possible to design a low-cost electrode with a renewable surface for the determination of sulfite through its electroreduction. In this context, carbon paste electrodes are made with multi-walled carbon nanotubes (MWCNTs) as highly conductive carbonaceous material and as binder, a mixture of mineral oil (MO) and an ionic liquid (IL) (N-octylpyridinium hexafluorophosphate). It allows the manufacture of high-conductivity electrodes, economical, easy to prepare, electrocatalytic, with a renewable surface, that act as excellent sensors in the detection and quantification of sulfite through its electrochemical reduction.

2. Results and Discussion

2.1. Obtaining and Characterization of MWCNT/IL/MO Carbon Paste Electrodes

Figure 1 shows the different morphologies of multiwalled carbon nanotubes bonded with ionic liquid and mineral oil (MWCNT/IL/MO), in a ratio of 70:20:10 (by mass), and on multiwalled carbon nanotubes only bound with mineral oil (MWCNT/MO), in a ratio of 70:30 (by mass). Figure 1 shows that the electrode that has IL in its structure (Figure 1B) has a higher resolution, clearly observing the nanotubes, due to its higher conductivity, compared to the electrode that only has mineral oil as a binder (Figure 1A).

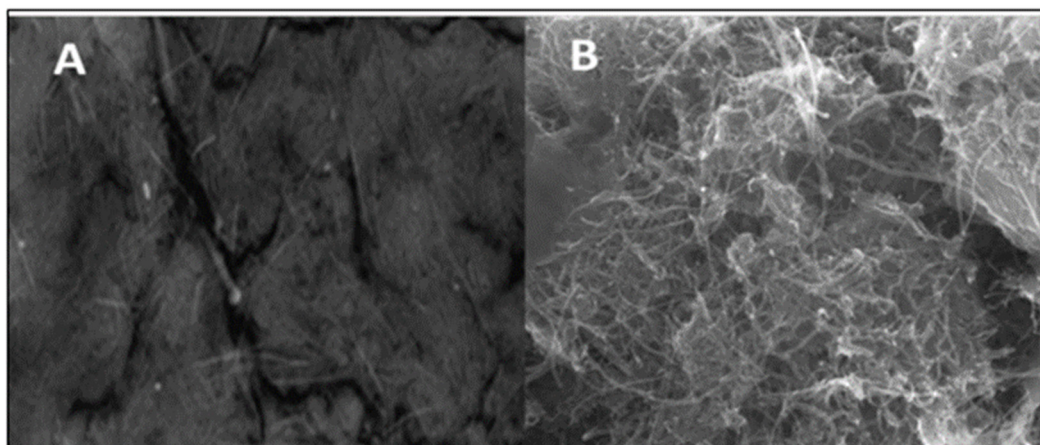


Figure 1. FESEM images of the (A) (MWCNT/MO) electrode, and (B) (MWCNT/IL/MO) electrode. Magnification: 40,000 \times .

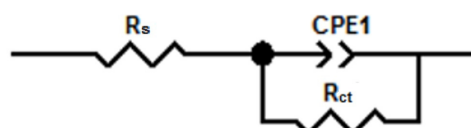
On the other hand, EDX studies were carried out to determine the chemical composition of each electrode, randomly selecting three areas in each case. The results are summarized in Table 1 and confirm the presence of ionic liquid $[\text{OPy}]^+[\text{PF}_6]^-$ on the electrode surface.

Table 1. Percentage values of weight for MWCNT/MO electrodes and MWCNT/IL/MO electrodes.

| Electrode | %C | %O | %F | %P |
|-------------|------------------|-----------------|-----------------|-----------------|
| MWCNT/MO | 96.81 ± 0.21 | 3.19 ± 0.26 | — | — |
| MWCNT/IL/MO | 93.55 ± 2.81 | 4.02 ± 0.12 | 1.53 ± 0.05 | 0.90 ± 0.03 |

2.2. Electrochemical Characterization of MWCNT/IL/MO Carbon Paste Electrodes

The electrical properties of MWCNT/IL/MO carbon paste electrodes in the presence of sulfite (5 mmol L^{-1} sulfite in BRB pH 1.81) have been studied using Electrochemical Impedance Spectroscopy (EIS). The equivalent circuit that fits the Nyquist diagram, recorded in the absence and presence of IL, is depicted in Scheme 1. In this circuit, R_s , CPE1, and R_{ct} represent the resistance of the solution, a constant phase element corresponding to double layer capacitance, and the resistance to charge transfer associated with sulfite reduction. For the electrode containing IL (see Figure 2), the diameter of the semicircle is reduced from 776.6Ω to 99.7Ω , confirming the electrocatalytic capacity of this electrode for sulfite reduction. At high frequencies, resistance to charge transfer appears and at low frequencies, diffusion processes are appreciated. Generally, the resistance to charge transfer (R_{ct}) of the electrode is equivalent to the diameter of the semicircle in the Nyquist plot [30]. Finally, the ohmic resistance of the solution (R_s) remains constant in the two paste electrodes in the presence of sulfite (see Table 2).



Scheme 1. Equivalent circuit for the carbon paste electrodes.

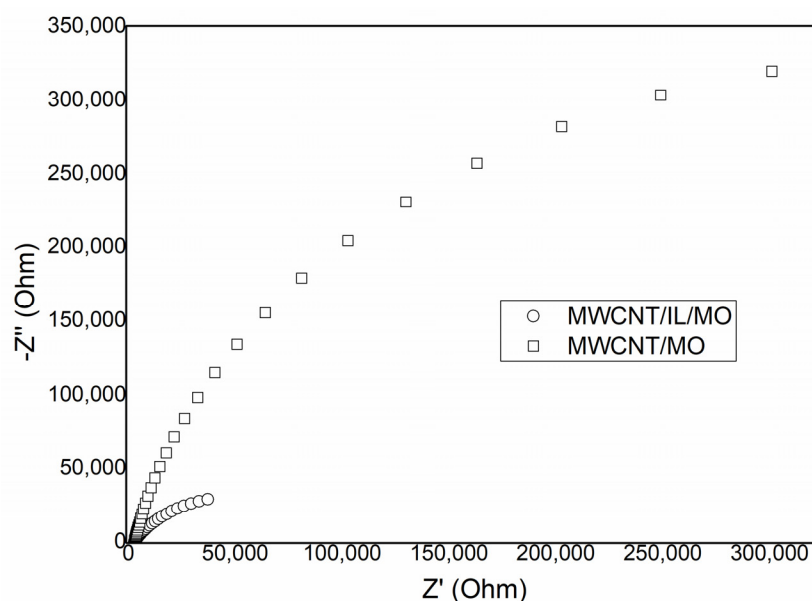


Figure 2. Nyquist diagram for the MWCNTIL/MO and MWCNT/MO systems in 5 mmol L⁻¹ solution of sulfite in BRB (pH 1.81). Frequencies: 100,000 Hz–1 Hz. Impedance performed at a potential of -0.5 V.

Table 2. Values of R_s , R_{ct} , and CPE obtained from the equivalent circuit of Scheme 1 for the paste electrodes.

| Paste Electrode | R_s (Ω) | R_{ct} (Ω) | CPE ($F\ cm^{-2}$) |
|-----------------|--------------------|-----------------------|----------------------|
| MWCNT/MO | 2926 | 776,610 | 0.89 |
| MWCNT/IL/MO | 2850 | 99,275 | 0.70 |

2.3. Electrochemical Behavior of Sulfite on MWCNT/IL/MO

Figure 3A shows a square wave voltammogram of the MWCNT/IL/MO electrode at different pHs in the presence of sulfite. Figure 3B shows the maximum cathodic currents (I_p) against pH variation. Both graphs indicate that the best pH for a catalytic reaction is near pH 2.

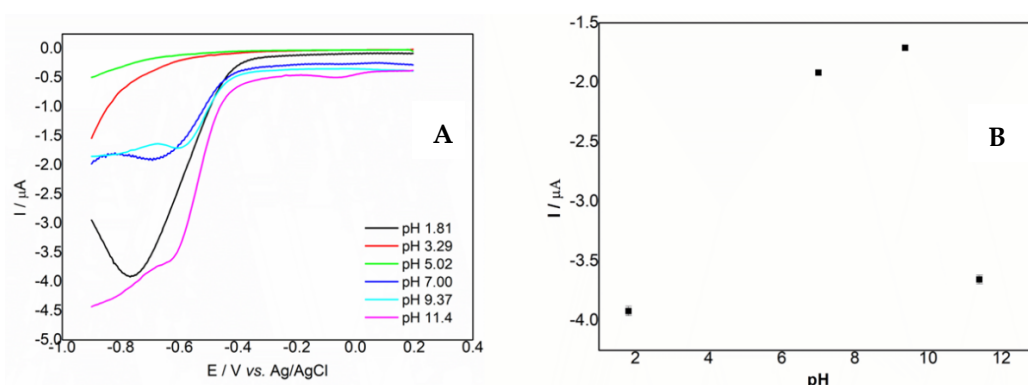


Figure 3. (A) Cyclic voltammetry profiles of MWCNT /IL/MO electrodes in presence of 5 mmol L⁻¹ sulfite in 0.04 mol L⁻¹ BRB, pH 1.81–11.4, in Ar. (B) Maximum cathodic current (I_p) vs. pH obtained from Figure 3A. The error bars represent the standard deviation of three independent measurements.

Considering that the best current response is observed in acid conditions, the sulfite reduction study is carried out at pH 1.81. This behavior is consistent with the chemical equilibrium of the sulfite species. At high pH values, the products of this equilibrium are

avored towards the formation of sulfurous acid, whereas in acid conditions, there is a higher concentration of dissolved SO_2 , which is the species that actually undergoes electrochemical reduction at the electrode surface. Therefore, the highest maximum cathodic currents are found in more acidic conditions. Based on these results, all electroanalytical studies were performed in a BRB pH 1.81 solution.

On the other hand, the electrochemical response of the electrode was studied in a potential range that goes from +0.2 V to -0.9 V vs. Ag/AgCl, and at a scan rate of 100 mV s^{-1} in the absence and presence of sulfite. Figure 4 presents the voltammetric profile for the MWCNT/MO and MWCNT/IL/MO electrodes in the absence and presence of 5 mmol L^{-1} of sulfite. The response of the analyte corresponds to the characteristic profile of the sulfite reduction. According to the previous literature, this reduction corresponds to the transformation of dissolved SO_2 into the radical anion SO_2^- [28,29]. MWCNT/IL/MO shows an E_p value for reduction of -0.56 V. When the electrode does not have IL, the voltammetric profile shows no signal and coincides with the blank, indicating that it is the IL that catalyzes the sulfite reduction (see Figure 4).

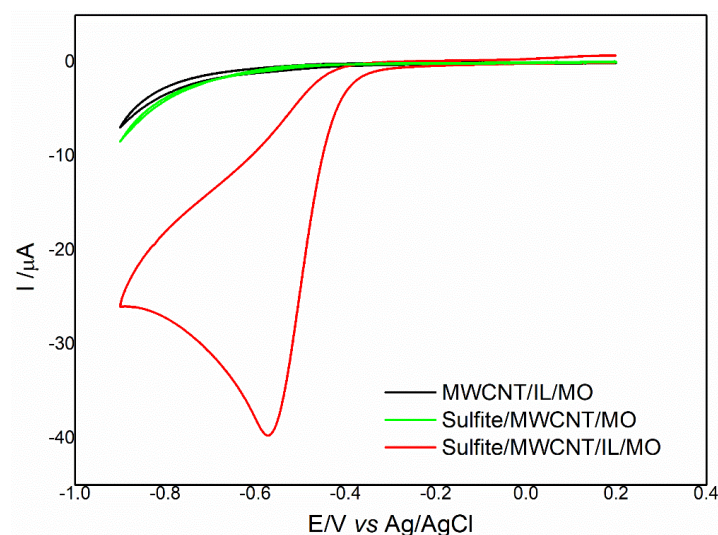


Figure 4. Cyclic voltammetry in absence (black line) and presence (red and green lines) of 5 mmol L^{-1} sulfite, in BRB (pH 1.81). Scan rate: 100 mV s^{-1} (1 cycle).

It is interesting to note that the edges of carbon nanotubes, generally very active for many reactions [31,32], are not active enough in this case to catalyze this reaction under the aforementioned conditions.

To calculate the number of electrons involved in this reaction, it is necessary to determine the electroactive area of the electrodes. For this, the effect of the scan rate (v) on the electrochemical behavior of a probe solution of ferri-ferrocyanide ions in an aqueous medium was measured (Figure 5). With these results, the electroactive area of the MWCNT/IL/MO electrode is calculated.

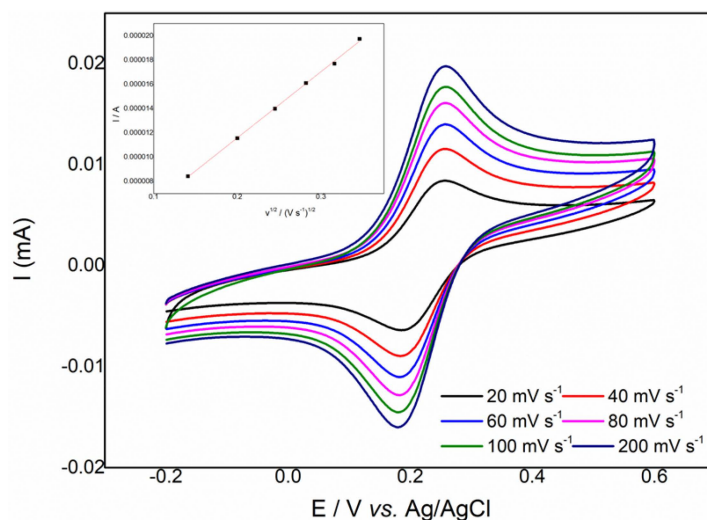


Figure 5. Cyclic voltammetry of the probe solution of ferri-ferrocyanide ions at different scan rates in NaNO_3 0.1 mol L^{-1} . Inset: variation of reduction peak current with square root of scan rate.

The results show that the peak current (I_p) increases linearly with the square root of the scan rate of the potential ($v^{1/2}$). The electroactive area is calculated from the slope of the linear regression curve ($R^2 = 0.99874$) (inset of Figure 5) using Equation (1):

$$\frac{I_p}{\sqrt{v}} = (2.65 \times 10^5) \times \sqrt{n^3} \times A \times \sqrt{D} \times C \quad (1)$$

where A is the electroactive area, n corresponds to the number of electrons transferred ($n = 1$), D is the diffusion coefficient of ferrocyanide $6.5 \times 10^{-6} \text{ cm}^2 \text{ s}^{-1}$, and C corresponds to the concentration ferrocyanide probe $5.0 \times 10^{-6} \text{ mol m}^{-3}$, obtaining a value of electroactive area $A = 0.016 \text{ cm}^2$.

Taking the electroactive area, the number of transferred electrons can be calculated through the equations and if the reaction is irreversible. The irreversibility of the reaction (mass transfer-controlled) is clearly observed in Figure 6.

$$I_p = 2.99 \times 10^5 n \sqrt{(1 - \alpha)n_\alpha} A \sqrt{D} C \sqrt{v} \quad (2)$$

$$\frac{0.0477 \text{ V}}{E_p - E_{p/2}} = (1 - \alpha)n_\alpha \quad (3)$$

$$E_p - E_{p/2} = -0.543 - (-0.461) = |0.082|$$

A corresponds to the electroactive area of the electrode (0.016 cm^2), and $(1 - \alpha)n_\alpha = 0.5817$ is obtained from Equation (3), where α is the transfer coefficient and n_α is the number of electrons transferred in the rate-determining step. The E_p value corresponds to 100 mV s^{-1} . D is the diffusion coefficient of the analyte [33] and C is the sulfite concentration ($5 \times 10^{-6} \text{ mol cm}^{-3}$). The number of electrons transferred in the reduction of sulfite (n) is obtained from the slope of the graph in Figure 6. Using Equation (2), $n = 0.5$ is obtained, which indicates that the electrochemical reduction of sulfite is a transfer process half an electron for sulfite. It has been described in the literature that the equilibrium anion radical SO_2^- dithionite is established very quickly, with dimerization rate constants close to those controlled by diffusion [33] at a pH close to 2, which explains the number of electrons found in this work.

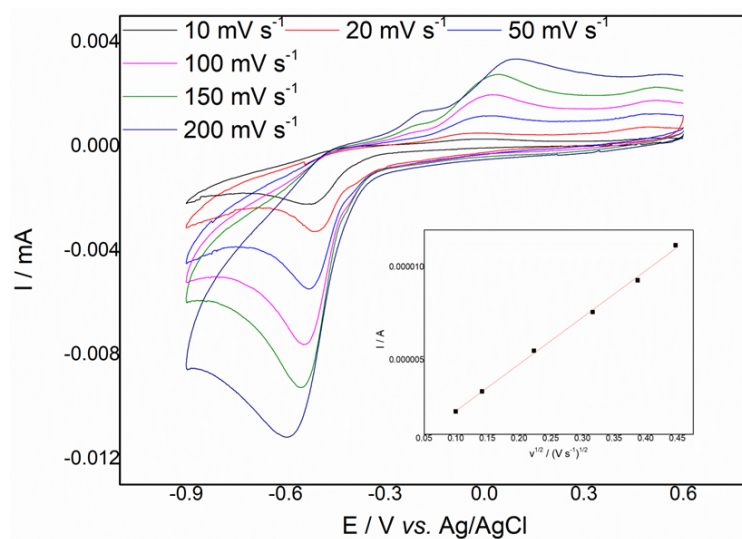


Figure 6. Cyclic voltammetry at different scan rate for the reduction of sulfite of 5 mmol L^{-1} in BRB (pH 1.81) on MWCNT/IL/MO.

2.4. Voltammetric Determination of Sulfite

A calibration curve of peak reduction current versus analyte concentration was prepared. The technique used was square wave voltammetry and the optimized parameters were the following: frequency = 50 Hz, amplitude = 0.025 V, increment = 0.004 V. The calibration curve (six replicates) was prepared with concentrations of $5 \pm 0.2 \text{ mmol L}^{-1}$, $10 \pm 0.3 \text{ mmol L}^{-1}$, $20 \pm 0.6 \text{ mmol L}^{-1}$, $30 \pm 0.8 \text{ mmol L}^{-1}$, and $50 \pm 1.5 \text{ mmol L}^{-1}$ of a certified standard of sodium sulfite at pH 1.81, at BRB (see Figure 7).

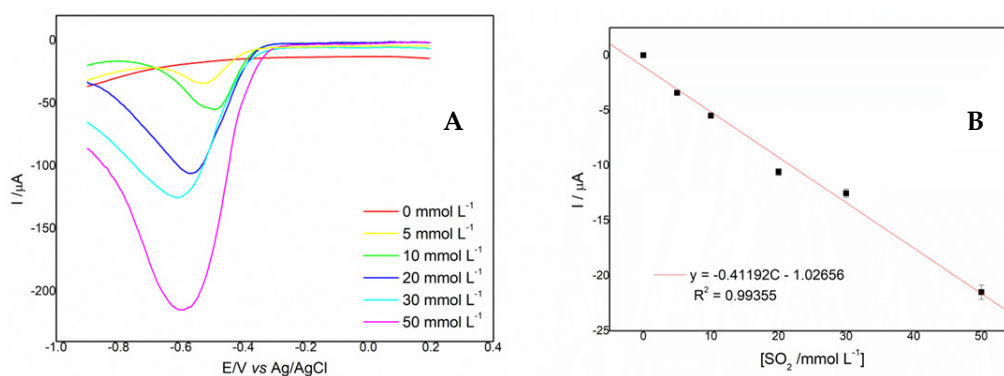


Figure 7. (A) Square wave voltammetry for the MWCNT/LI/AM electrode at different concentrations of sodium sulfite. (B) Linear regression obtained.

2.5. Analytical Parameters

Figure 7 shows the voltammetric response of the electrode at different of sulfite. The linear regression of I_{p_c} versus sulfite concentration $R^2 = 0.99355$.

The calibration curve of sulfite in MWCNT/IL/MO is linear in the range of 5.0 mmol L^{-1} to 50 mmol L^{-1} , with a limit of detection of $1.6 \pm 0.05 \text{ mmol L}^{-1}$ ($102.5 \text{ mg SO}_2 \text{ L}^{-1}$) ($S/N = 3$). It is noted that the limit of detection of the MWCNT/IL/MO system $1.6 \pm 0.05 \text{ mmol L}^{-1}$ is higher compared to other published studies [22,34]. This value indicates that with this system, it could be detected below the maximum concentrations established for sulfite present in some alcoholic beverages ($200\text{--}300 \text{ mg L}^{-1}$) [9]. In addition, the simplicity of the sulfite detection method is highlighted.

The linear regression equation is: $I (\mu\text{A}) = 1.02656 + 0.41192 C (\text{mmol L}^{-1})$. The sensitivity is $0.41192 \mu\text{A mmol}^{-1} \text{ L}$.

From these data we obtain that MWCNT/IL/MO electrode exhibits a one order of magnitude range of linear concentration, a lower limit of detection, and a higher sensitivity compared to most of electrochemical sulfite sensors reported [22,28,29,34].

Another important electroanalytical study is repeatability. The electrochemical response of four (MWCNT/IL/MO) paste electrodes was assessed, with different triplicate, performed the same day at pH 1.81 in BRB, using a concentration of sodium sulfite equivalent to $5 \pm 0.2 \text{ mmol L}^{-1}$. The relative standard deviation (RSD) of the peak current response for the four different electrodes was of 3.55% ($n = 3$), demonstrating that the MWCNT/IL/MO sensor presents good repeatability (Figure 8).

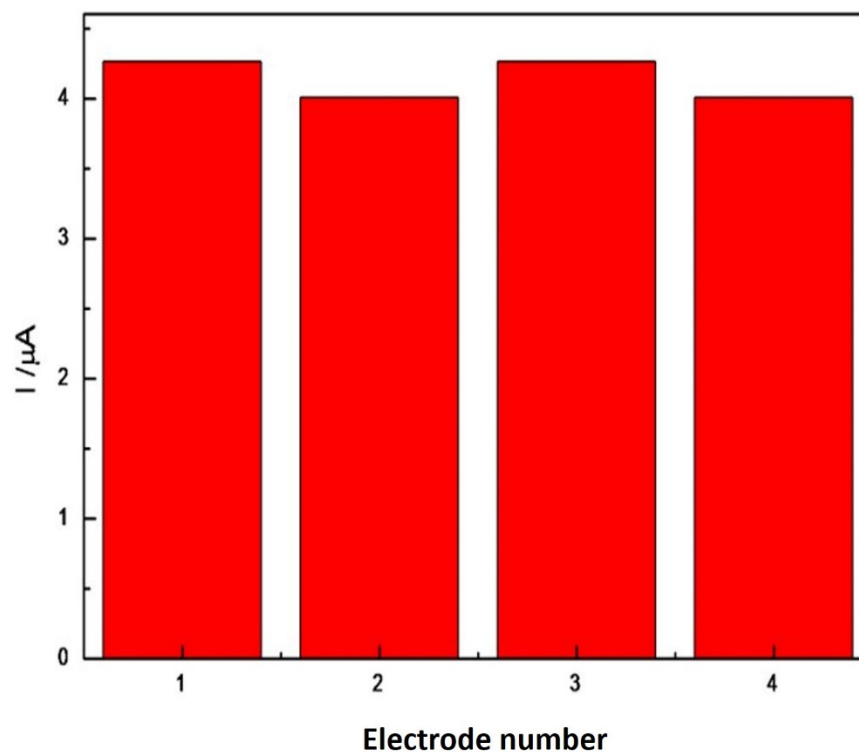


Figure 8. Repeatability study for four electrodes.

3. Experimental

3.1. Materials, Reagents, and Equipment

Multi-walled carbon nanotubes (MWCNTs), diethyl ether (DEE), and potassium chloride (KCl) were purchased from Merck (Santiago, Chile) and used as received. Acetic acid (CH_3COOH), boric acid (H_3BO_3), orthophosphoric acid (H_3PO_4), mineral oil (MO), sodium sulfite (98% pure), certified sulfite standard, potassium ferricyanide ($\text{K}_3[\text{Fe}(\text{CN})_6]$) (98.5% pure), and potassium ferrocyanide trihydrate ($\text{K}_4[\text{Fe}(\text{CN})_6]$) were purchased from Sigma Aldrich (Santiago, Chile), and used as received. Ultrapure water ($>17 \text{ M}\Omega\text{-cm}$) was obtained from a Direct-Q[®] water purification system (Model ZRQSV3WW) and argon gas (99.99% pure) was purchased from AGA (Santiago, Chile). N-octylpyridinium hexafluorophosphate $[\text{OPy}]^+[\text{PF}_6]^-$ ionic liquid was previously synthesized and characterized [35,36] obtaining a yield of 91%.

Electrochemical studies were performed in a conventional three-electrode electrochemical cell which contains: an Ag/AgCl ($3 \text{ mol L}^{-1} \text{ KCl}$) reference electrode (RE), a platinum wire counter electrode (CE), and a hollow Teflon working electrode (WE) of 2 mm diameter, which is filled with the carbon pastes specified in Table 1. The cell contains a 0.1 mol L^{-1} Britton–Robinson (BRB) buffer aqueous solution, and the pH is adjusted by additions of $5 \text{ mol L}^{-1} \text{ NaOH}$ and $5 \text{ mol L}^{-1} \text{ HCl}$. The solution is maintained in an inert atmosphere of Ar.

Morphological characterization was performed using a JEOL 6300 scanning electron microscope (SEM) coupled to 6699 ATW X-ray microanalysis elemental system (Oxford Instruments Ltd., Abingdon, UK). Data were analyzed using the associated software (version 4.0). Spectra were recorded using a 15 keV accelerating voltage. Cyclic voltammetry (CV), square wave voltammetry (SWV) and electrochemical impedance spectroscopy (EIS) were performed using a model 750D workstation (CH Instruments, Austin, TX, USA). All measurements were performed at room temperature, 21 ± 1 °C.

3.2. Paste Electrode Preparation

The 70:30 (*w/w*) ratio of carbon materials and binder was used after experimentally checking that at different binder ratios (both higher and lower), the electrodes lose their mechanical and structural consistency. For the manufacture of carbon paste electrode, the bare carbon paste electrode was made by mixing MWCNT and oil mineral in a 70:30 percent weight-to-weight ratio [37]. On the other hand, to manufacture the carbon paste electrode with MWCNT binder with oil mineral and ionic liquid, a 70:20:10 (*w/w*) ratio of MWCNT, oil mineral, and ionic liquid was used, respectively.

The 70: 30 (*w/w*) ratio of carbon and binder materials was used after experimentally verifying that at different binder ratios (both higher and lower), the electrodes lose their mechanical and structural consistency. For the fabrication of the carbon paste electrode, the bare carbon paste electrode was fabricated by mixing MWCNT and mineral oil in a 70:30 percent weight-to-weight ratio [35]. On the other hand, for the fabrication of the MWCNT binder carbon paste electrode with mineral oil and ionic liquid, a ratio of 70:20:10 (*w/w*) of MWCNT, mineral oil, and ionic liquid, respectively, was used. The mixtures are homogenized in a mortar by adding diethyl ether. After homogenization, the diethyl ether is evaporated until a carbon paste is obtained. The generated paste is used to fill hollow Teflon electrodes. After compacting by hand, the electrodes are left at 90 °C in an oven. After 2 h, the electrodes are cooled to room temperature and polished with weighing paper to a smooth surface. The obtained electrodes were electrochemically stabilized by cycling the potential in the range of 200 to −900 mV in BRB pH 1.81. The obtained electrodes were characterized by their voltammetric response using the potassium ferrocyanide/potassium ferricyanide redox couple, showing that they are very reproducible systems.

4. Conclusions

This work shows that the electrode prepared with carbon nanotubes bonded with a mixture of LI (N-octylpyridinium hexafluorophosphate) and mineral oil allows obtaining an electrode that is easy to prepare, low-cost, and eco-friendly. The electrode is active for the reduction of sulfite, being able to become a sensor to determine its concentration in an acid medium.

Author Contributions: Methodology, M.B.V., J.I. and V.C.; investigation, L.G. and M.J.A.; writing—original draft preparation, L.G. and M.J.A.; writing—review and editing, G.R. and R.A. All authors have read and agreed to the published version of the manuscript.

Funding: This work was funded by Regular-UNAB project N° DI-010-22/REG, ANID FONDECYT N° 1220107, ANID FONDECYT POSTDOCTORADO N° 3220040, and Millenium Institute on Green Ammonia as Energy Vector MIGA, ANID/Millennium Science Initiative Program/ICN2021_023.

Data Availability Statement: Not applicable.

Conflicts of Interest: The authors declare no conflict of interest.

References

1. Inetianbor, J.; Yakubu, J.; Ezeonu, S. Effects of food additives and preservatives on man-a review. *Asian J. Sci. Technol.* **2015**, *6*, 1118–1135.
2. Ruiz-Capillas, C.; Jiménez-Colmenero, F. Application of flow injection analysis for determining sulphites in food and beverages: A review. *Food Chem.* **2009**, *112*, 487–493. [[CrossRef](#)]

3. Isaac, A.; Davis, J.; Livingstone, C.; Wain, A.J.; Compton, R.G. Electroanalytical methods for the determination of sulfite in food and beverages. *TrAC Trends Anal. Chem.* **2006**, *25*, 589–598. [[CrossRef](#)]
4. Gupta, M.K.; Basavaraj, G. Sulphites in food & drinks in asthmatic adults & children: What we need to know. *Indian J. Allergy Asthma Immunol.* **2021**, *35*, 43.
5. Vally, H.; Misso, N.L. Adverse reactions to the sulphite additives. *Gastroenterol. Hepatol. Bed Bench* **2012**, *5*, 16.
6. Lacava, A. Fadugba, Sulfite hypersensitivity: A case of asthma triggered by sulfites. *Ann. Allergy Asthma Immunol.* **2020**, *125*, S98. [[CrossRef](#)]
7. Galil, A.; Kumar, Y.; Sathish, M.A.; Nagendrappa, G. Simple spectrophotometric method for the determination of sulfur dioxide by its decolorizing effect on the peroxovanadate complex. *Anal. Chem.* **2008**, *63*, 239–243.
8. Rankine, B.C.; Pocock, K.F. Alkalimetric determination of sulphur dioxide in wine. *Aust. Wine Brew. Spirit Rev.* **1970**, *29*, 40–44.
9. Zamora, F. *Elaboración y Crianza del Vino Tinto: Aspectos Científicos y Prácticos*; AMV Ediciones, Mundi-Prensa: Madrid, Spain, 2003.
10. Monier-Williams, G.W. Determination of Sulphur Dioxide in Foods. In *Public Health and Medical Subjects Report No. 43*; Ministry of Health: London, UK, 1927; pp. 415–416.
11. Wang, M.; Guo, L.; Cao, D. Amino-Functionalized Luminescent Metal–Organic Framework Test Paper for Rapid and Selective Sensing of SO₂ Gas and Its Derivatives by Luminescence Turn-On Effect. *Anal. Chem.* **2018**, *90*, 3608–3614. [[CrossRef](#)]
12. Al-Hosney, H.A.; Grassian, V.H. Water, sulfur dioxide and nitric acid adsorption on calcium carbonate: A transmission and ATR-FTIR study. *Phys. Chem. Chem. Phys.* **2005**, *7*, 1266–1276. [[CrossRef](#)]
13. Baltrusaitis, J.; Cwiertny, D.M.; Grassian, V.H. Adsorption of sulfur dioxide on hematite and goethite particle surfaces. *Phys. Chem. Chem. Phys.* **2007**, *9*, 5542–5554. [[CrossRef](#)] [[PubMed](#)]
14. Zheng, J.; Tan, F.; Hartman, R. Simple spectrophotometry method for the determination of sulfur dioxide in an alcohol-thionyl chloride reaction. *Anal. Chim. Acta* **2015**, *891*, 255–260. [[CrossRef](#)] [[PubMed](#)]
15. Wu, K.; Guo, J.; Wang, C. Dispersible and discrete metalloporphyrin-based CMP nanoparticles enabling colorimetric detection and quantitation of gaseous SO₂. *Chem. Commun.* **2014**, *50*, 695–697. [[CrossRef](#)] [[PubMed](#)]
16. Carrascon, V.; Ontañón, I.; Bueno, M.; Ferreira, V. Gas chromatography-mass spectrometry strategies for the accurate and sensitive speciation of sulfur dioxide in wine. *J. Chromatogr. A* **2017**, *1504*, 27–34. [[CrossRef](#)]
17. Koch, M.; Köppen, R.; Siegel, D.; Witt, A.; Nehls, I. Determination of total sulfite in wine by ion chromatography after in-sample oxidation. *J. Agric. Food Chem.* **2010**, *58*, 9463–9467. [[CrossRef](#)]
18. Zenga, R.-F.; Lan, J.-S.; Wu, T.; Liu, L.; Lui, Y.; Ho, R.; Ding, Y.; Zhang, T. A novel mitochondria-targeted near-infrared fluorescent probe for selective and colorimetric detection of sulfite and its application in vitro and vivo. *Food Chem.* **2020**, *318*, 126358–126365. [[CrossRef](#)]
19. Sung, Q.; Zhang, W.; Qian, J. A ratiometric fluorescence probe for selective detection of sulfite and its application in realistic samples. *Talanta* **2017**, *162*, 107–113.
20. Chandra, S.; Rachna, R. Determination of sulfite, with emphasis on methods of biological detection: A review. Department of Biochemistry, University of Maryland. *Bioanal. Chem.* **2013**, *405*, 2599–2608.
21. Dinçkaya, E.; Sezgintürk, M.K.; Akyılmaz, E.; Ertaş, F.N. Sulfite determination using sulfite oxidase biosensor based glassy carbon electrode coated with thin mercury film. *Food Chem.* **2007**, *101*, 1540–1544. [[CrossRef](#)]
22. Silva, E.M.; Takeuchi, R.M.; Santos, A.L. Carbon nanotubes for voltammetric determination of sulphite in some beverages. *Food Chem.* **2015**, *173*, 763–769. [[CrossRef](#)]
23. Ahmed, M.I.; Aziz, M.A.; Helal, A.; Shaikh, M.N. Direct electrodeposition of nanogold on gallium-doped zinc oxide by cyclic voltammetry and constant-potential techniques: Application to electro-oxidation of sulfite. *J. Electrochem. Soc.* **2016**, *163*, D277. [[CrossRef](#)]
24. Moghaddam, H.M.; Malakootian, M.; Beitollah, H.; Biparva, P. Nanostructured base electrochemical sensor for determination of sulfite. *Int. J. Electrochem. Sci.* **2014**, *9*, 327–341.
25. Kovaleva, S.; Aksinenko, O.; Korshunov, A. Electrooxidation of sulfite ions on a composite carbon-containing electrode modified with submicron gold particles. *J. Anal. Chem.* **2020**, *75*, 1348–1357. [[CrossRef](#)]
26. Dadamos, T.R.; Teixeira, M.F. Electrochemical sensor for sulfite determination based on a nanostructured copper-salen film modified electrode. *Electrochim. Acta* **2009**, *54*, 4552–4558. [[CrossRef](#)]
27. Isaac, A.; Wain, A.J.; Compton, R.G.; Livingstone, C.; Davis, J. A novel electroreduction strategy for the determination of sulfite. *Analyst* **2005**, *130*, 1343–1344. [[CrossRef](#)]
28. Ordeig, O.; Banks, C.E.; Del Campo, F.J.; Muñoz, F.X.; Davis, J.; Compton, R.G. Sulfite determination at in situ plated copper modified gold ultramicroelectrode arrays. *Electroanal. Int. J. Devoted Fundam. Pract. Asp. Electroanal.* **2006**, *18*, 247–252. [[CrossRef](#)]
29. Montes, R.H.; Richter, E.M.; Munoz, R.A. Low-potential reduction of sulfite at a ruthenium-oxide hexacyanoferrate modified electrode. *Electrochem. Commun.* **2012**, *21*, 26–29. [[CrossRef](#)]
30. Yu, H.; Feng, X.; Chen, X.X.; Wang, S.S.; Jin, J. A highly sensitive determination of sulfite using a glassy carbon electrode modified with gold nanoparticles-reduced graphene oxide nanocomposites. *J. Electroanal. Chem.* **2017**, *801*, 488–495. [[CrossRef](#)]
31. Wildgoose, G.G.; Banks, C.E.; Leventis, H.C.; Compton, R.G. Chemically modified carbon nanotubes for use in electroanalysis. *Microchim. Acta* **2006**, *152*, 187–214. [[CrossRef](#)]
32. Roldan Luna, S.M. Supercondensadores Basados en Electrolitos Redox Activos. Ph.D. Thesis, Departamento de Ciencia de los Materiales e Ingeniería Metalúrgica de la, Universidad de Oviedo, Asturias, Spain, 2013.

33. Streeter, I.; Wain, A.J.; Davis, J.; Compton, R.G. Cathodic reduction of bisulfite and sulfur dioxide in aqueous solutions on copper electrodes: An electrochemical ESR study. *J. Phys. Chem. A* **2005**, *109*, 18500–18506. [[CrossRef](#)]
34. Winiarski, J.P.; Reginato de Barros, M.; Magosso, H.A.; Jost, C.L. Electrochemical reduction of sulfite based on gold nanoparticles/silsesquioxane-modified electrode. *Electrochim. Acta* **2017**, *251*, 522–531. [[CrossRef](#)]
35. Gidi, L.; Honores, J.; Arce, R.; Arévalo, M.C.; Aguirre, M.J.; Ramírez, G. Enhanced Electrocatalysis of the Oxygen Reduction Reaction Using Cobalt and Iron Porphyrin/Ionic Liquid Systems. *Energy Technol.* **2019**, *7*, 1900698. [[CrossRef](#)]
36. Domańska, U.; Skiba, K.; Zawadzka, M.; Padaszyńska, K.; Królikowska, M. Synthesis, physical, and thermodynamic properties of 1-alkyl-cyanopyridinium bis((trifluoromethyl)sulfonyl)imide ionic liquids. *J. Chem. Thermodyn.* **2013**, *56*, 153–161. [[CrossRef](#)]
37. Figueiredo-Filho, L.C.; Brownson, D.A.; Gómez-Mingot, M.; Iniesta, J.; Fatibello-Filho, O.; Banks, C.E. Exploring the electrochemical performance of graphitic paste electrodes: Graphene vs. graphite. *Analyst* **2013**, *138*, 6354–6364. [[CrossRef](#)]